JACS
JOURNAL OF THE AMERICAN CHEMICAL SOCIETY
Communication
pubs.acs.org/JACS

Silicon Ring Strain Creates High-Conductance Pathways in Single-Molecule Circuits

Timothy A. Su,[†] Jonathan R. Widawsky,[‡] Haixing Li,[‡] Rebekka S. Klausen,[†,§] James L. Leighton,*[,†] Michael L. Steigerwald,*[,†] Latha Venkataraman,*[,‡] and Colin Nuckolls*[,†]

[†]Department of Chemistry, Columbia University, New York, New York 10027, United States
[‡]Department of Applied Physics, Columbia University, New York, New York 10027, United States

Supporting Information

ABSTRACT: Here we demonstrate for the first time that strained silanes couple directly to gold electrodes in break-junction conductance measurements. We find that strained silicon molecular wires terminated by alkyl sulfide aurophiles behave effectively as single-molecule parallel circuits with competing sulfur-to-sulfur (low G) and sulfur-to-silacycle (high G) pathways. We can switch off the high conducting sulfur-to-silacycle pathway by altering the environment of the electrode surface to disable the Au–silacycle coupling. Additionally, we can switch between conductive pathways in a single molecular junction by modulating the tip–substrate electrode distance. This study provides a new molecular design to control electronics in silicon-based single molecule wires.

This manuscript unveils the characteristics of strained silicon in single molecule electrical devices. Current state-of-the-art integrated circuits incorporate strain in the silicon crystal lattice to improve charge mobility and channel conductance. As electronic devices continue their ultra-miniaturization,[1−5] understanding the effects of strain in molecular versions of silicon will be crucial. In this study, we incorporate the strained silacyclobutane ring into a molecular wire (**1**) to investigate how silicon ring strain manifests in molecular conductance. Previously, we found that permethylated oligosilanes with alkyl sulfide contacts at both ends of the molecule conduct through a single pathway from sulfur to sulfur.[6] Here, we demonstrate that silane **1** conducts not only from sulfur to sulfur (red, low G pathway) but also from sulfur to silacycle (blue, high G pathway). The latter pathway arises as a consequence of the significant strain of the silacycle. Additionally, we find that we can control the pathway through which conductance occurs and thereby switch between two distinct conductance states.

We synthesize **1** from 1,1-dichlorosilacyclobutane and 4-(methylthio)phenylmagnesium bromide (synthetic details and characterization are described in the Supporting Information (SI)). We grew single crystals suitable for X-ray diffraction from methanol vapor diffusion into a solution of **1** in 1,2,4-trichlorobenzene (TCB). The bond angle about the aryl carbons and silicon atom describes a standard tetrahedron (109°) while the silacyclobutane ring is significantly distorted (CH_2–Si–CH_2, 79°). We measure single-molecule conductance using a scanning tunneling microscope-based break-junction (STM-BJ) technique.[7] Point contacts between the Au tip and substrate electrodes are repeatedly broken and formed in a solution of the target molecule at room temperature and low voltage (225 mV). After the Au–Au point contact is broken, aurophilic thiomethyl groups[8] on the molecule bind to undercoordinated gold atoms to form Au–molecule–Au junctions. Conductance (current/voltage) is measured across the gap as a function of tip–substrate displacement (Δx), and the resulting traces reveal molecule-dependent plateaus signifying junction formation with conductance values below G_0 ($2e^2/h$), the quantum of conductance describing a single Au–Au contact.[9] Junctions form and break thousands of times, and we analyze the measured traces using one- and two-dimensional histograms[10] as detailed below.

The results from STM-BJ measurement of **1** in 1,2,4-trichlorobenzene demonstrate four unique characteristics that are unlike any molecule we have ever measured. First, as we see from a two-dimensional conductance-displacement histogram shown in Figure 1a, we have two distinct conductance states that differ by an order of magnitude. This difference is significantly greater than we previously observed for 4,4′-bipyridine.[11] We define the region around 4.2×10^{-4} G_0 as the high G state and the region around 4.0×10^{-5} G_0 as the low G state. Sample conductance traces have plateaus at these conductance values, as shown in the inset. Second, we note that both high and low G states occur directly after the Au–Au contact rupture ($\Delta x = 0$); yet, a high G junction can only sustain a 0.4 nm elongation while a low G junction can sustain a 0.6 nm elongation. Since junction elongation length correlates with the conduction path length,[12] we hypothesize the conduction path in the high G state is shorter than in the low G state.

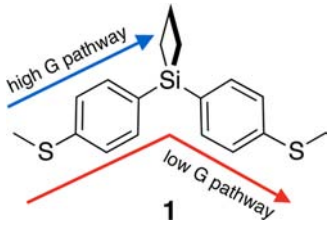

1

Received: October 17, 2013
Published: November 21, 2013

   dx.doi.org/10.1021/ja410656a | J. Am. Chem. Soc. 2013, 135, 18331−18334

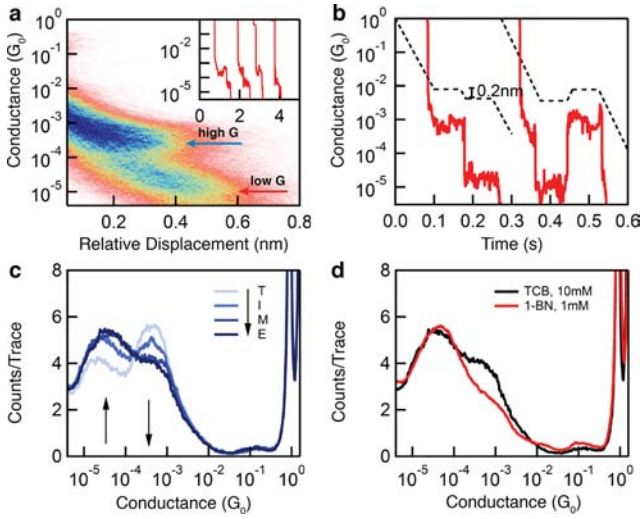

Figure 1. (a) 2D histogram of the first 5000 traces of **1** (1 mM TCB) with selected sample traces (inset). (b) Single-junction elongation (left) and compression traces (right) showing switching events. The black dotted line denotes the piezoelectric motion while the red solid line shows the conductive response. (c) 1D histogram tracking sequential sets of 5000 traces (20 000 total) to show peak evolution with increasing concentration. (d) 1D histogram of **1** in 1-BN solvent (1 mM), compared with TCB (10 mM).

Third, we find that we can induce switching from the high to low *G* state reliably; however, the reverse occurs infrequently (see SI for more detailed analysis). To switch from a high to low *G* state (elongation), we first form a high *G* junction and then pull the junction an additional 0.2 nm as shown in Figure 1b. We find that, with this modified ramp, 65% of the traces switch from high to low *G*, 12% stay in high *G*, and 23% break. To switch from low to high *G*, we form a low *G* junction, then compress the electrodes by 0.2 nm. The fraction of traces that switch from low to high *G* is small (13%). Under compression, the majority of measured traces remain in the low *G* state, indicating that the high *G* state is not easily accessible once the low *G* state is formed.

The fourth and most surprising distinction between **1** and other molecular wires demonstrating multiple conductance states[11−13] is that the ratio between the high and low *G* states is concentration-dependent. The one-dimensional conductance histogram in Figure 1c shows that as solvent evaporates over time, the high *G* peak diminishes as the low *G* peak grows in. This effect is reversible: replenishing the solvent subsequent to evaporation restores the initial peak distribution (Figure S1). We find the high *G* peak is more intense in dilute solutions (1 mM) whereas the low *G* peak is more intense in concentrated solutions (10 mM) in both trichlorobenzene and trimethoxybenzene solvents (Figures S2 and S3). At 1 mM in 1-bromonapthalene (1-BN) however, the high *G* peak is conspicuously absent (Figure 1d, red).

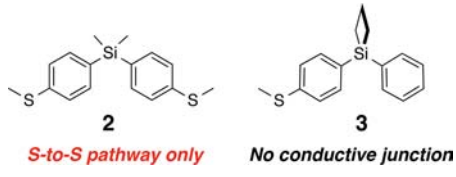

We attribute the low *G* state in **1** to sulfur-to-sulfur conductance because its conductance-displacement profile is nearly identical to that of dimethylsilane **2** (Figure S4).[6] We hypothesize that the high *G* state represents a junction where current flows between one of the sulfides and the silacycle (Figure 2a). This junction geometry is consistent with the shorter elongation length of the high *G* state. Furthermore, it explains the lack of the high *G* peak in 1-bromonapthalene. We have previously shown that 1-bromonaphthalene binds much more strongly to undercoordinated Au sites relative to chlorinated and ethereal solvents.[14] Accordingly, the absence of the high *G* state suggests that bromonapthalene molecules are preventing the formation of the weak Au−silacycle contact in the high *G* geometry. This Au−silacycle interaction must also be weaker than the Au-SMe linkage because the low *G* state is unaffected in the 1-BN experiment. Indeed, we find that the Au−silacycle conduit is too fragile to form on its own, as monosulfide **3** has no measurable conductance (Figure S5). The secondary Au−SMe linkage is therefore necessary to organize the silacycle onto a nearby Au atom. Because the Au−silacycle interaction is easily disrupted, the high *G* state only occurs if the Au atoms that span the auxiliary sulfide and silacyclobutane linkages are uncoordinated, thus explaining the concentration dependence in trichlorobenzene: at high concentrations, there are significantly more Au atoms coordinated by stronger sulfide linkages and, therefore, a lower probability that the high *G* junction geometry can be accessed (Figure 2b).

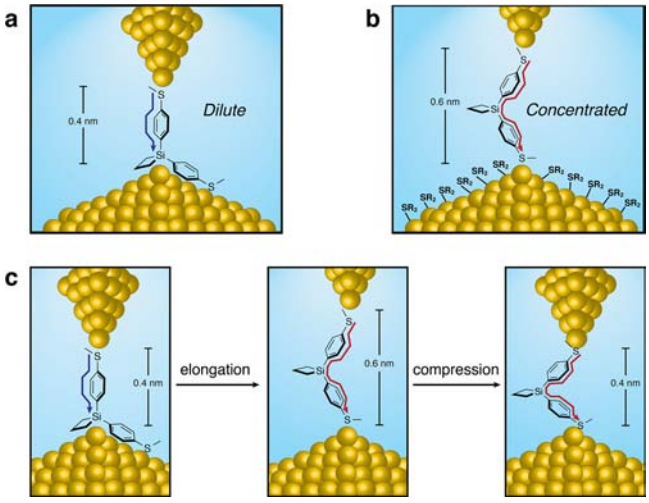

Figure 2. (a) In dilute conditions, an auxiliary sulfur group organizes the Au−silacycle conduit. (b) At higher concentrations, more molecules assemble on the electrode surface and the weak Au−silacycle conduit is more easily displaced. (c) A schematic explaining the nonadiabatic nature of single-junction switching.

The switching statistics from the elongation and compression experiments are also consistent with this explanation. Switching from high to low *G* is frequent (65%) because the molecule is easily pulled out of the Au−silacycle interaction to the more stable low *G* conformer at Δx = 0.6 nm. Switching from low to high *G* is less frequent (13%) because there is poor incentive to form the Au−silacycle complex, as there are other geometries the low *G* state can adopt at Δx = 0.4 nm (Figure 2c). This model for our high *G* state is also supported by the findings of others[15,16] who have shown that ethynyltrimethylsilanes form self-assembled monolayers on gold surfaces through Au−silane interactions.

dx.doi.org/10.1021/ja410656a | J. Am. Chem. Soc. 2013, 135, 18331−18334

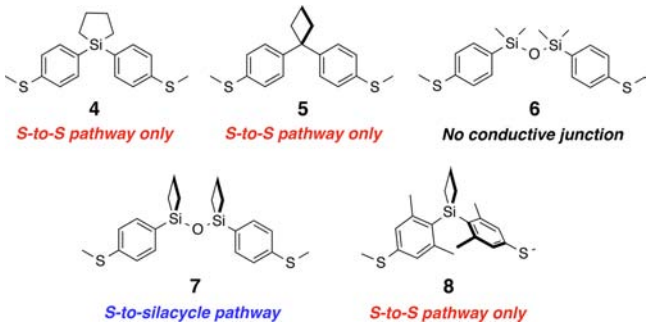

The Au−silane conduit observed here is specific to highly strained silicon rings. The STM-BJ measurement of less strained silacyclopentane **4** (CH_2−Si−CH_2, 96° [DFT-calculated; see SI]) gives a single conductance peak at 5.1 × 10^{-5} G_0 corresponding to the low G state and analogous to dimethylsilane **2** (Figure S6). We also find this high G state is not a generality of strained four-membered rings. All-carbon cyclobutane analog **5** gives a single conductance peak (1.7 × 10^{-4} G_0) close in magnitude to that for bis((4-methylthio)-phenyl)methane (1.2 × 10^{-4} G_0 (Figure S7)). Cyclobutane **5** is significantly strained, with a ring angle of 87° in the crystal structure. The fact that cyclobutane **5** does not yield a secondary conductance state highlights a fundamental difference between carbon and silicon: though **1** and **5** are structurally analogous, the electronics of strained silicon enables coupling between the gold electrode and silacycle.

Conductance in these molecular systems typically occurs through tunneling, which is strongly distance dependent.[5] The Au−silacycle interaction provides a shorter conduit relative to the distal methyl sulfide, thereby enabling high conductance even in structures that do not typically conduct. Previously we demonstrated that tetramethyldisiloxane **6** does not form conductive junctions because the oxygen atom disrupts delocalization across the molecule in the orbital most commonly ascribed to S-to-S conductance (HOMO).[6] DFT calculations show that the HOMO of bis(cyclobutyl)disiloxane **7** is similarly localized on one end of the molecule (SI). We find that disiloxane **7** gives a high G peak (2.5 × 10^{-4} G_0) that strongly diminishes with increasing concentration (Figure S8). These results can be rationalized if the silacycle is an electronic contact that opens an alternative conductance pathway.

We find that steric encumbrance near the silacyclobutane disables the Au−silacycle interaction and suppresses the high G state. We install *ortho*-methyl groups in silacyclobutane **8** to simultaneously frustrate arene rotation[17,18] and restrict the Au−silane interaction. Accordingly, the STM-BJ measurement of **8** yields a single, sharp, low G peak (7.6 × 10^{-5} G_0, Figure S9). We can also tune the high G state's sensitivity to concentration by modifying the structure of the gold-molecule chelate. Butyl-linked **9** gives both high (3.1 × 10^{-4} G_0) and low G (1.8 × 10^{-5} G_0) peaks at 1 mM (Figure 3a). As solvent evaporates, the high G peak in **9** disappears entirely (darkest blue line) and resembles the analogous dimethylsilane **10** (2.6 × 10^{-5} G_0). This is in contrast with **1**, where the high G state is still accessible at higher concentrations. Like **1**, we find the high G peak in **9** re-emerges when solvent is replenished. These molecules demonstrate that the behavior of the high G state—whether it diminishes completely or does not appear at all, can be tuned by changing the linker structure.

To elucidate the conductance mechanism in these monosilane systems (and particularly the strained silanes), we

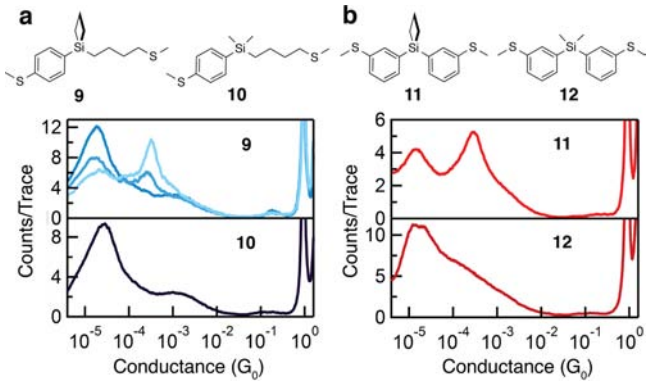

Figure 3. 1D histograms of **9** and **10**; (b) **11** and **12**. (a) For **9**, the lightest line compiles the first 2000 traces while the darkest line compiles the last 2000 traces over 15 000 traces.

synthesized **11** and **12** with *meta*-thioanisole linkers. Previous studies have shown that molecular wires with *meta*-substituted linkers are poor π-conductors due to quantum interference effects,[19−22] in which the nodes at the *meta*-position prevent the distal sulfur pπ orbitals from coupling through the molecule. Our own investigations of oligoenes,[21] inorganic clusters,[23] fluorenes,[24] and longer silanes (Figure S10) have shown that while molecules with *para*-substituted thioanisole linkers strongly conduct, *meta*-substituted linkers yield little to no conductance. In the monosilanes studied here, we find that the magnitude of conductance is not significantly affected by whether the thioanisole linkers are *para*- or *meta*-substituted. *Meta*-linked **11** gives two sharp conductance peaks (2.7 × 10^{-4} G_0, 1.4 × 10^{-5} G_0) similar to the high and low G states for **1** (Figures 3b, S11). Dimethylsilane analog **12** furnishes a single peak (1.7 × 10^{-5} G_0) similar to the low G state in **11**. Conductance in **11** and **12** implies the σ-framework is the dominant conduit for diarylmonosilanes. The presence of the high G state in **11** further suggests the strained silane 'shorts' end-to-end conductance.

The silacyclobutane family is useful in silicon-directed organic synthesis. The Lewis acidity at the silicon center activates an array of organic transformations that are otherwise difficult to achieve with unstrained silanes.[25−27] This Lewis acidity implies that the Si−C bond is strongly polarized toward the carbon. We speculate that it is these vicinal carbons or polarized Si−C bonds that contact the gold electrode and propose that the Lewis acidic properties of silacyclobutanes in organic reaction chemistry manifest here as a new conductance state. Drawing such an analogy between reaction chemistry and molecular electronics opens the possibility that the vast store of synthetic methodology can be applied to create new types of molecular devices.

We demonstrate here for the first time that strained silanes couple directly to gold electrodes. This coupling enables strained silicon molecular wires with alkyl sulfide leads to conduct through two distinct pathways: sulfur-to-sulfur and sulfur-to-silacycle. We find that the molecular wire 'chooses' its conductive pathway based on the surface environment of the Au electrodes. Furthermore, we can controllably switch from the high to low G state in a single junction by modulating the tip−substrate distance. Our studies here uncover the electronic effects of straining silicon at the molecular level and provide a foundation for the realization of strained silicon molecular components.

dx.doi.org/10.1021/ja410656a | J. Am. Chem. Soc. 2013, 135, 18331−18334

■ ASSOCIATED CONTENT

Supporting Information

Synthetic procedures, STM-BJ procedures, table of conductances, additional figures, characterization data, computational details, and crystallographic data (CIF). This material is available free of charge via the Internet at http://pubs.acs.org.

■ AUTHOR INFORMATION

Corresponding Authors

leighton@chem.columbia.edu
mls2064@columbia.edu
lv2117@columbia.edu
cn37@columbia.edu

Present Address

[§]Department of Chemistry, The Johns Hopkins University, Baltimore, MD 21218, USA.

Notes

The authors declare no competing financial interest.

■ ACKNOWLEDGMENTS

The STM-BJ experiments were supported as part of the Center for Re-Defining Photovoltaic Efficiency Through Molecular-Scale Control, as Energy Frontier Research Center funded by the U.S. Department of Energy (DOE), Office of Science, Office of Basic Energy Science under Award Number DE-SC0001085. T.A.S. is supported by the NSF Graduate Research Fellowship under Grant No. 11-44155. H.L. is supported by the Semiconductor Research Corporation and New York CAIST program. J.L.L. acknowledges support from NSF Grant CHE-11-52949. We thank Arunabh Batra for helpful discussions and Dr. Yasuhiro Itagaki for mass spectrometry assistance. We thank the NSF (CHE-0619638) for acquisition of an X-ray diffractometer and Dr. Wesley Sattler and Serge Ruccolo for crystallographic analysis of **1** and **5**.

■ REFERENCES

(1) Aviram, A. *J. Am. Chem. Soc.* **1988**, *110*, 5687.
(2) Joachim, C.; Gimzewski, J. K.; Aviram, A. *Nature* **2000**, *408*, 541.
(3) Heath, J. R.; Ratner, M. A. *Phys. Today* **2003**, *56*, 43.
(4) Nitzan, A.; Ratner, M. A. *Science* **2003**, *300*, 1384.
(5) Tao, N. J. *Nat. Nanotechnol.* **2006**, *1*, 173.
(6) Klausen, R. S.; Widawsky, J. R.; Steigerwald, M. L.; Venkataraman, L.; Nuckolls, C. *J. Am. Chem. Soc.* **2012**, *134*, 4541.
(7) Xu, B.; Tao, N. J. *Science* **2003**, *301*, 1221.
(8) Park, Y. S.; Whalley, A. C.; Kamenetska, M.; Steigerwald, M. L.; Hybertsen, M. S.; Nuckolls, C.; Venkataraman, L. *J. Am. Chem. Soc.* **2007**, *129*, 15768.
(9) Agraït, N.; Rodrigo, J.; Vieira, S. *Phys. Rev. B* **1993**, *47*, 12345.
(10) Kamenetska, M.; Koentopp, M.; Whalley, A.; Park, Y.; Steigerwald, M.; Nuckolls, C.; Hybertsen, M.; Venkataraman, L. *Phys. Rev. Lett.* **2009**, *102*, 126803.
(11) Quek, S. Y.; Kamenetska, M.; Steigerwald, M. L.; Choi, H. J.; Louie, S. G.; Hybertsen, M. S.; Neaton, J. B.; Venkataraman, L. *Nat. Nanotechnol.* **2009**, *4*, 230.
(12) Meisner, J. S.; Kamenetska, M.; Krikorian, M.; Steigerwald, M. L.; Venkataraman, L.; Nuckolls, C. *Nano Lett.* **2011**, *11*, 1575.
(13) Li, C.; Pobelov, I.; Wandlowski, T.; Bagrets, A.; Arnold, A.; Evers, F. *J. Am. Chem. Soc.* **2008**, *130*, 318.
(14) Fatemi, V.; Kamenetska, M.; Neaton, J. B.; Venkataraman, L. *Nano Lett.* **2011**, *11*, 1988.
(15) Marchenko, A.; Katsonis, N.; Fichou, D.; Aubert, C.; Malacria, M. *J. Am. Chem. Soc.* **2002**, *124*, 9998.
(16) Marqués-González, S.; Yufit, D. S.; Howard, J. K.; Martín, S.; Osorio, H. M.; García-Suárez, V. M.; Nichols, R. J.; Higgins, S. J.; Cea, P.; Low, P. J. *Dalton Trans.* **2013**, *42*, 338.
(17) Vonlanthen, D.; Rotzler, J.; Neuburger, M.; Mayor, M. *Eur. J. Org. Chem.* **2010**, *2010*, 120.
(18) Venkataraman, L.; Klare, J. E.; Nuckolls, C.; Hybertsen, M. S.; Steigerwald, M. L. *Nature* **2006**, *442*, 904.
(19) Ke, S.; Yang, W.; Baranger, H. U. *Nano Lett.* **2008**, *8*, 3257.
(20) Solomon, G. C.; Andrews, D. Q.; Goldsmith, R. H.; Hansen, T.; Wasielewski, M. R.; Van Duyne, R. P.; Ratner, M. A. *J. Am. Chem. Soc.* **2008**, *130*, 17301.
(21) Aradhya, S. V; Meisner, J. S.; Krikorian, M.; Ahn, S.; Parameswaran, R.; Steigerwald, M. L.; Nuckolls, C.; Venkataraman, L. *Nano Lett.* **2012**, *12*, 1643.
(22) Guédon, C. M.; Valkenier, H.; Markussen, T.; Thygesen, K. S.; Hummelen, J. C.; van der Molen, S. J. *Nat. Nanotechnol.* **2012**, *7*, 305.
(23) Roy, X.; Schenck, C. L.; Ahn, S.; Lalancette, R. A.; Venkataraman, L.; Nuckolls, C.; Steigerwald, M. L. *Angew. Chem., Int. Ed.* **2012**, *51*, 12473.
(24) Klausen, R. S.; Widawsky, J. R.; Su, T. A.; Li, H.; Chen, Q.; Steigerwald, M. L.; Venkataraman, L.; Nuckolls, C., unpublished results.
(25) Myers, A. G.; Kephart, S. E.; Chen, H. *J. Am. Chem. Soc.* **1992**, *114*, 7922.
(26) Denmark, S. E.; Griedel, B. D.; Coe, D. M. *J. Org. Chem.* **1993**, *58*, 988.
(27) Matsumoto, K.; Oshima, K.; Utimoto, K. *J. Org. Chem.* **1994**, *59*, 7152.